Second Scientific Conference on Modern Technologies in Oil Refining In 14-16/5/2013

Hydroisomerization and Hydrocracking of n-Heptane over Nanoporous Trimetallic (Pt-Ni-Co/SBA-15 Catalyst)

Talib M.Albayati
Department of Chemical Engineering, University of Technology/Baghdad
Email:talib_albyati@yahoo.com
Aidan M. Doyle
Division of Chemistry and Environmental Science, Manchester Metropolitan University, Chester St., Manchester, M1 5GD, United Kingdom.

ABSTRACT

The heterogeneous hydroisomerization and hydrocracking of n-heptane was carried out within the pores of the mesoporous SBA-15 silicas, within which was encapsulated trimetallic nanoparticles of Pt-Ni-Co. The structural and textural features of the nanoporoussilicas, both with and without encapsulated nanoparticles, were characterised using small angle X-ray diffraction, scanning electron microscopy (SEM), EDAX, nitrogen adsorption-desorptionporosimetry/BET surface area analysis,Fourier-transform infrared (FTIR) spectroscopyand transmission electron microscopy (TEM).

Catalytic testing was conducted using a plug-flow reactor in a catalyst testing rig under tightly controlled conditions of temperature, reactant flow rate and pressure.Species were leaving the reactor andanalysed by Gas Chromatography. The results show thatPt-Ni-Co/SBA-15 had a high activity for conversion of n-heptane (around 85%). The catalyst was found to be stable to heating and did not undergo any significant deactivation during reaction at temperatures up to 400 °C.

Keywords: Nanoporous Material; SBA-15;N-Heptane;Trimetallic Catalyst; Hydroisomerization; Hydrocracking

عملية ألأزمرة والتكسيرالحراري للهبتان الاعتيادي فوق العامل المساعد النانوي المسامي ثلاثي المعادن (Pt-Ni-Co/SBA-15)

الخلاصة

ان عملية الازمرة والتكسير الحراري للهبتان الاعتيادي في تفاعلات غير متجانسة (متباينة) الاطوار وبوجود العامل المساعد قد حدثت ضمن مسامات المادة النانوية المسامية SBA-15 التي تم حشوتها بجسيمات او جزيئات المعادن النانوية الثلاثية 1% (البلاتين-النيكل-الكوبلت). ان تركيب المادة النانوية المسامية SBA-15 ومميزات السطح الخارجي لها تم دراستها بواسطة الاشعة السينية XRD بالاضافة الى دراسة المسح الالكتروني المجهريSEM وتحليل نسبة العناصرEDAX. وكما تم قياس المساحة السطحية وقطر المسامات بواسطة غاز النيتروجين بعملية الامدصاص وازالة الامدصاصBET . بالاضافة الى قياس المجاميع الفعالة FT-IR

وكذلك تم استخدام المجهر الالكتروني الناقل (TEM). ان جميع هذه الخصائص تم دراستها قبل وبعد عملية التحميل بالمعادن.ان عملية اختبار العامل المساعد قد اجريت في المفاعل الانبوبي وفي ظروف مسيطرة عليها مثل الضغط ، درجة الحرارة، ومعدل التدفق. النتائج اظهرت ان فعالية تقييم العامل المساعد في المفاعل الانبوبي توحي بان المعادن الثلاثية المحملة (Pt-Ni-Co)/SBA-15 1% لها فعالية عالية اثناء تحويل الهبتان الاعتيادي بحدود 85% في المفاعل الانبوبي.
اوجدت النتائج استقرارية العامل المساعد للتسخين ولم يخضع لاي عملية تعطيل مؤثرة في درجة حرارة التفاعل لحد 400 درجة مئوية.

الكلمات المرشدة: المواد النانوية المسامية :SBA-15 : الهبتان الاعتيادي : عامل مساعد ثلاثي المعادن: الازمرة: التكسير الحراري.

INTRODUCTION

The hydroisomerization of linear paraffins, especially the n-alkanes present in light naphtha streams (C_5 and C_6), into corresponding branched isomers is a considerable interest in the petroleum industry, because these branched compounds possess higher research octane number (RON) [1–3]. Hydroisomerization of C_5 and C_6 linear paraffins is not a new process, this was developed in the 1960s [4–7]. Nowadays, even though several licensers such as UOP, IFP, and Exxon, Mobil, and Mitsubishi, offer hydroisomerization process for naphtha (C_6–C_9), this technology requires improvement in the activity, selectivity, and stability of the catalyst. Generally, the hydroisomerization reaction is always followed by a hydrocracking reaction. This latter reaction is favored for long linear paraffins (>C_6) and multibranchedparaffins [8, 9].

The interest in the production of clean gasolines with high octane numbers has led to the search for new solid catalysts with improved selectivity for *n*C_7isomerization [10-12]. Therefore, many efforts have been devoted to seeking effective catalysts which can promote the selectivity of the branched paraffins in the hydroisomerization of paraffins with the chain-length longer than C_6 [13, 14]. A great variety of supports have been investigated, such as silica [15], silica-alumina [16], activated carbon [17], MCM-41[18], SBA-15[19], zeolites [20-22], and so on.

It has been widely accepted that this reactions are achieved over bifunctional catalysts consisting of noble metal particles supported on a matrix which contains acid sites [23]. The major reactions promoted by bifunctional catalysts are hydrogenation, dehydrogenation, isomerization, cyclization and hydrocracking [24]. In the last decade, researchers paid more attention to hydroconversion of alkanes over solid acid catalysts with large pore diameter including mesoporous molecular sieves in order to prepare new catalysts for the conversion of heavier hydrocarbons [25]. Among them, mesoporous molecular sieves which possess the acidic sites and good hydrothermal stability are favored.

Zhao et al. [26, 27] extended the family of highly ordered mesoporous silicates by synthesizing Santa Barbara Amorphous (SBA) type materials. Since its discovery in 1998, SBA-15 has attracted considerable attention as a potential catalyst support, adsorbent, hydrogen storage, and drug delivery media, and as a

hard template for other nanostructure materials [28] because of its remarkably high thermal stability and variable pore size. SBA-15 possesses high surface area in the range of 600–1000 m^2 g^{-1} and consists of hexagonal arrays of cylindrical channels with tunable pore diameters between 5 and 30 nm. Micropores located inside the pore walls interconnect these channels. Moreover, SBA-15 exhibits higher thermal and hydrothermal stability and thicker pore walls 2-8 nm [29] as shown in Figure (1).

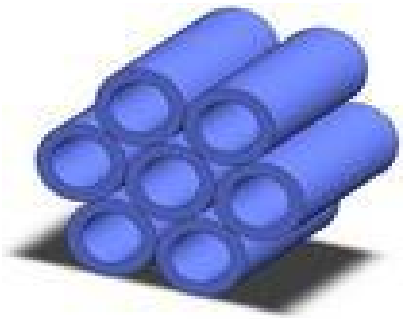

Figure (1) Schematic diagram for structure of SBA [30].

However, no more studies have so far been reported in the open literature on the use of Nanoporoustrimetallic catalysts for isomerization and reforming processes of n-Heptane. In this work, we have investigated the catalytic activities of 1% (Pt-Ni-Co) catalysts supported on SBA-15 for the reaction of n-heptane inHydroisomerization and Hydrocracking reactions.

EXPERIMENTAL

Chemicals

All chemicals viz. triblock copolymer poly (ethylene glycol)- Block-poly (propylene glycol)-block-poly (ethylene glycol) (Pluronic P123, molecular weight = 5800, $EO_{20}PO_{70}EO_{20}$), tetraethyl orthosilicate(TEOS; purity > 98 %) as a silica source), hydrochloric acid (HCl), Pt $(NH_3)_4Cl2.H_2O$(99.99 %), $CoN_2O_6.6H_2O$ (99.99 %), and Ni $(NO3)_2.6H_2O$(99.99 %), (99%) were purchased from Aldrich Chemical Inc., n-Heptane's (purity of 99.33 wt.%:Sigma-Aldrich). All chemicals were used as received without further purification. Millipore water was used in all experiments.

Synthesis of SBA-15

Mesoporous silica SBA-15 silica was prepared using the conventional methods [26]. Syntheses were performed using triblock copolymer, poly (ethylene glycol)-block-poly (propylene glycol)-block-poly (ethylene glycol) (PEG–PPG–PEG),(6g) Pluronic P123 (triblock co-polymer, EO20PO70EO20, MW=5800) as the structure directing agent was obtained from BASF and dissolved into deionized water (45 g) and 2 M HCl (180 g) while stirring at 35-40 ^{0}C for 20 min. After that tetraethyl orthosilicate (TEOS) as the silica source under acidic conditions (12.8 g) was added to the solution, stirring continued for 20 h. Then, the mixture was aged at 90 ^{0}C in a Teflon bottle for 24h under static conditions. The resulting white powder was obtained by filtration and purified via washing with ethanol and deionized

water. The purified product was calcined at 550 Cº for 12h using a heating ramp rate 2 °C/min. [31].

Preparation of Metals Support SBA-15 Mesoporous Catalyst

SBA-15 sampleswere metal-loaded by the method of incipient wetness impregnation (IWI) with $Pt(NH_3)_4Cl_2.H_2O$ as a platinum precursor, $Ni(NO_3)_2.6H_2O$ as a nickel precursorand $Co(NO_3)_2.6H_2O$ as a cobalt precursor. Impregnation solutions were prepared by dissolving the appropriate amount of metals (1% loading) is introduced into 0.1 M HCl solvent to load metallic with a total of 1 wt% Pt, Ni and Co for the trimetallic catalyst. In order to achieve a high metal dispersion and inhibit agglomeration of the salt during the vaporization of the solvent, the total volume of the solution was equal to that of the used pore volume of the support. After impregnation, the catalysts were dried overnight in air at ambient temperature, then 24 h at 120 ºC, and finally calcined at 550 ºC for 4 h so as to get 1% (PtNi-Co)/SBA-15 catalyst.

Characterization

The small-angle XRD patterns were recorded under ambient conditions on a MiniFlex (Rigaku) diffractometer with Cu Kα radiation (λ = 1.5406Å). The X-ray tube was operated at 40 kV and 30 mA while the data were recorded in the 2θ range of 0.5–8° with a 2θ step size of 0.01 and a step time of 10s. The d-spacing and unit cell parameters were calculated using the formulas, $n\lambda = 2d\sin\theta$ and $\alpha_o = 2d100/\sqrt{3}$. Nitrogen adsorption/desorption measurements were conducted using a Micrometrics ASAP 2020 pore analyzer by N_2physisorption at -196ºC. Samples were degassed for 3 h at 350 ºC under vacuum ($p < 10^{-5}$ mbar) in the degas port of the sorption analyzer. The BET specific surface areas of the samples were calculated using the Brunauer–Emmett–Teller (BET) method in the range of relative pressures between 0.05 and 0.35. The pore size distributions were calculated from the desorption branch of the isotherm using the thermodynamics-based Barrett–Joyner–Halenda (BJH) method. The total pore volume was determined from the adsorption branch of the N_2 isotherm as the amount of liquid nitrogen adsorbed at $P/P_0 = 0.995$. The pore wall thickness (t_W) was calculated from the unit cell parameter (α_o) and pore size diameter (d_P). Mean mesopore diameters for the various samples were estimated from the nitrogen sorption data using BET analysis (4V/A). The infrared spectra (FT- IR) of the solid samples, diluted in (8 wt. %) KBr were recorded at room temperature in transmission mode in the range of 4000 to 400 cm^{-1} at 4 cm^{-1} resolution regions using, NICOLET 380 FT-IR spectrometer. The macropore structure was characterized by scanning electron microscopy (SEM), performed on a JEOL (JSM-5600 LV) scanning electron microscope. EDAX used in combination with SEM is an analytical technique which forms an elemental analysis of the catalyst to identify the chemical composition. Transmission electron microscopy (TEM) using a Titan TEM microscopeTEM is a common method used in analysing the size and distribution of metal clusters on a catalyst surface.

Catalytic test

To prepare for experiments, 0.1 g of each catalyst was pressed and sieved to the required size of 250-425 μm, loaded into a cylindrical fixed bed Pyrex micro-reactor of 4 mm ID and 400 mm length and held in place in the reactor by glass wool. The catalysts were calcined in air and reduced in H_2 in situ with 50 ml min^{-}

$^1H_2$ at 450 ºC for 4 h. The maximum temperature and heating rate of 450 ºC and 1 ºC min^{-1} applied during activation are set to avoid sintering and agglomeration of the metal on the catalyst and therefore gain maximum catalyst performance. Gas H_2 feed was passed through a saturator containing n-Heptanes (99.33 wt %, Sigma-Aldrich). The H_2 and n-C_7 flow rates ranged from 20-45 ml.min^{-1} and 0.287–0.686 ml.min^{-1} respectively and the experimentally determined molar composition of n-C_7 in the feed was 1.436 mol % and was calculated from extrapolated response factor values of n-C_7 by testing the feed total area on the GC-FID for blank runs across flow rates of 20–72 ml min^{-1}. This compared well to the theoretical molar composition calculated from the standard vapour pressure of n-C_7 at 0 ºC and confirms the saturator is working very close to the theoretical optimum for a range of H_2 flow rates. The catalysts were tested at atmospheric pressure, and temperatures ranging from 250-400 ºC. All gas productswere analysed using a Varian 3400 GC-FID fitted with a 50 m x 0.32 mm ID Plot Al_2O_3 capillary column.

RESULTS AND DISCUSSION

Characterization of the synthesized materials

The XRD patterns of SBA-15 samples before and after modification Figure (2) all displayed an intense diffraction peak at about 2θ of 0.9◦, which is characteristic of a mesostructure. Moreover, two additional peaks were observed in the XRD patterns, which can be indexed as (1 1 0) and (2 0 0) reflections of a hexagonal P6mm symmetry [32]. The results demonstrate that the periodic ordered structure of SBA-15 was maintained after modification.However, spacing values (a_o) of the grafted SBA-15 samples reduced somewhat see Table (1), compared to SBA-15, indicating changes in their wall thickness and pore size due to the deposition of loaded metals.

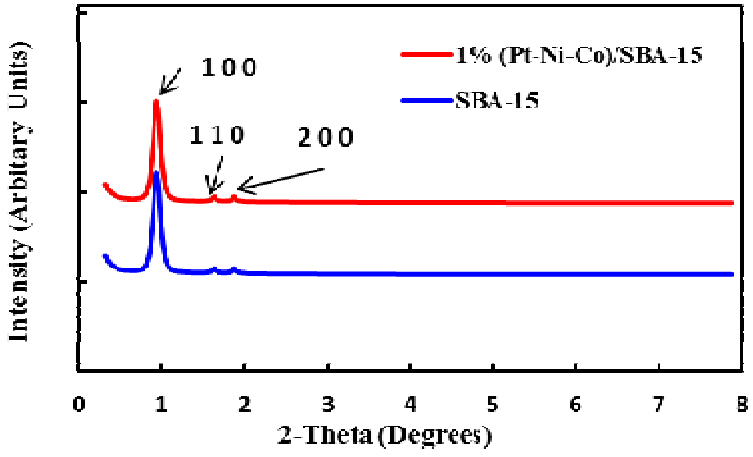

Figure (2) X-ray diffraction patterns of (SBA-15) and 1% (Pt-Ni-Co/SBA-15) supported catalyst.

Table (1) physicochemical properties of SBA-15 and 1% (Pt-Ni-Co/SBA-15) supported catalyst.

Sample	S_{BET} (m^2/g)	V_P (cm^3/g)	$V_{\mu P}$ (cm^3/g)	D_P (nm)	a_o(nm)	t_{wall} (nm)
SBA-15	901	1.88	0.07	8.5	11.08	2.58
1% (Pt-Ni-Co) / SBA-15	735	1.09	0.08	6.05	10.62	4.57

*S_{BET} is the surface area determined by using the BET method between the relative pressures (P/P0) 0.05–0.25. VP and $V_{\mu P}$ are respectively, the total pore volume and micropore volume obtained using the t-plot method. The total pore volume was estimated from the amount adsorbed at a relative pressure of 0.97. DP is the pore diameter calculated by means of the BJH method from the adsorption branch of the isotherm. a_o is the unit cell parameter calculated by XRD, being $a_o = 2d100/\sqrt{3}$. t_{wall} is the wall thickness calculated using the equation $t_{wall} = a_o - D_P$ [33].

The nitrogen adsorption isotherms of SBA-15 and grafted1% (Pt-Ni-Co)/SBA-15 materials had similar patterns as a type IV isotherm and a hysteresis loop type H1 Figure (2); hysteresis loops with sharp adsorption and desorption branches are indicative of a narrow pore size distribution. Figure (3) also shows that the nitrogen adsorbed amount decreases as SBA-15 is grafted with loaded metals. The structural parameters calculated from nitrogen adsorption measurements are presented in Table (1). In the table, it is shown that the specific surface area, pore volume, and pore size of the samples followed the order: SBA-15 >1% (Pt-Ni-Co)/SBA-15, whereas the different order was observed in terms of wall thickness.The significant decreases in the surface area of the loaded samples in comparison with SBA-15 confirm the attaching of supported metals groups inside the pores.

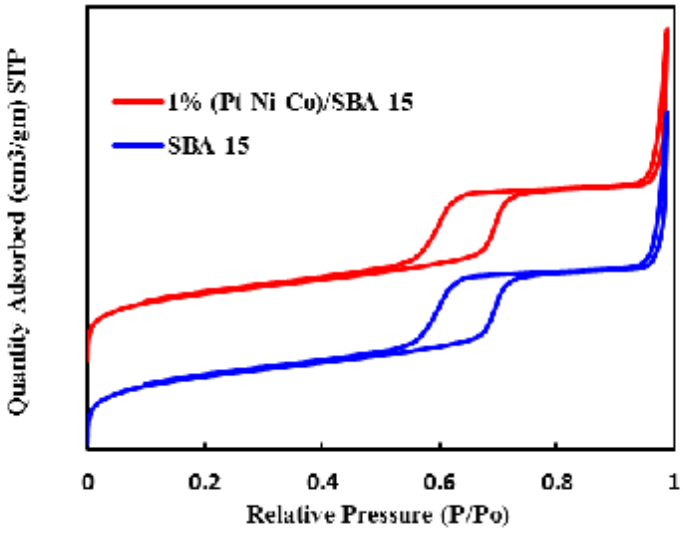

Figure (3) Nitrogen adsorption isotherms for SBA-15 and 1% (Pt- Ni-Co)/SBA-15 samples.

Figure (4) illustrates the pore size distribution (PSD) of SBA-15 and 1wt% (Pt-Ni-Co)/SBA-15 catalysts, samples prepared using incipient wetness impregnation

methods. The pore size of pure silica SBA-15 was 8.5 nm, obtained from N2 physisorption using the BJH method, while the pore size of 1wt% (Pt-Ni-Co)/SBA-15 was 6.05 nm. The catalyst shows a narrow PSD similar to SBA-15, indicating that the pore structure has not significantly altered. However, all catalysts show a bimodal PSD, with the first peak centered at around 55Å. This suggests that in these cases, there may be partial pore blockage or deposition of metals particles against the internal silica walls and/or at the pore apertures. The decrease of the pore diameter after metals grafting is mostly the result from the reconstruction due to dehydroxylation rather than additional layer of metala formed on the inside of the silica wall. This is evident in Table 1. There are three important points that can be highlighted: (i) the volume of adsorbed N_2decreased with increasing metalscontent, (ii) the portion of pores with diameter around 5 nm increased as the metals content increased and (iii) the presence of bimodal PSD indicates that metals oxide species have formed inside the pores [34].

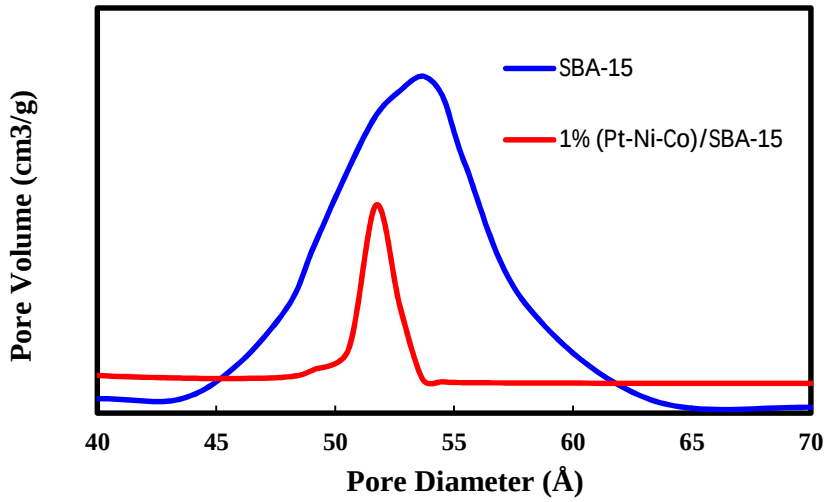

Figure (4) BJH pore size distribution (PSD) for SBA-15 and 1% (Pt-Ni-Co)/SBA-15 catalyst.

Figure (5) shows the FT-IR spectra of SBA-15 and the various catalysts. The spectra of all the materials contain the typical Si–O–Si bands around 1078, 804 and 455 cm^{-1}, which arise from the Si O Si stretching vibration. The absorption band at around 960 cm^{-1} can be assigned to either Si OH or Si O Si stretching vibrations. The broad band at around 3400 cm^{-1} is due to the presence of surface OH groups with strong H-bonding interactions between them. Finally the band at around 1631 cm^{-1} can be assigned to the deformation modes of OH bonds of adsorbed H_2O [35]. A loaded metal exhibits a very similar spectrum to SBA-15 due to its low metals content, whereas Ni-SBA-15 and Pt-SBA-15 exhibits two additional bands at 660 and 570 cm^{-1} (black arrows). These latter bands can be ascribed to metals vibrations in the cobalt oxide lattice. The (Pt-Ni-Co)/SBA bands for metals are slightly more intense than for SBA-15. We attribute this to the presence of larger

Particles on the external surface of the pores for (Pt-Ni-Co)/SBA-15 also exhibitsthe same absorbance bands, with progressively increasing intensity [36]. However even without incorporated Al, SBA-15 still displays some acidic properties. It is evident from this graph of the presence of Lewis sites on SBA-15 which promote dehydrogenation and hydrocracking reactions due to the formation of silanol groups during the calcination process of the catalyst [37].

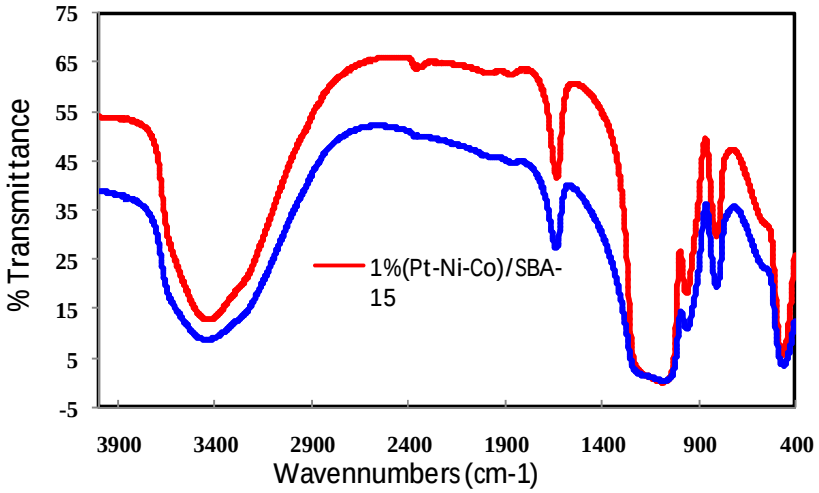

Figure (5) FT-IR spectra of SBA-15 and 1% (Pt-Ni-Co)/SBA-15.

SEM and EDAX of catalysts

SEM and EDAX characterisation techniques were performed on the prepared catalyst samples prior to testing. SEM images of SBA-15and (Pt-Ni-Co)/SBA-15 can be seen in Figure 5 and Figure 6 at magnifications of 10,000 for both of them. The surface morphology for SBA-15 and 1% (Pt-Ni-Co)/SBA-15 samples are very similar; however the 1% (Pt-Ni-Co)/SBA-15 catalyst particles are much bigger than those of the SBA-15.

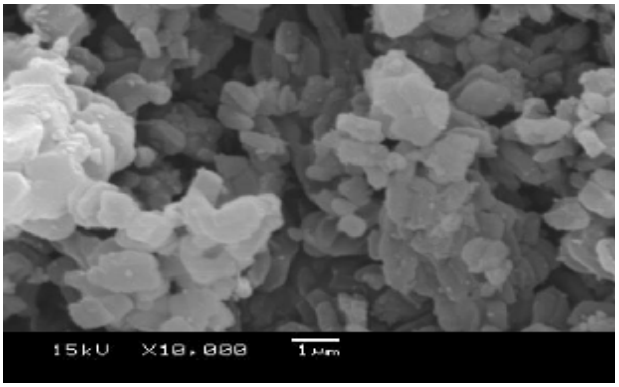

Figure (6) SEM image of SBA-15 ata magnification of 10,000.

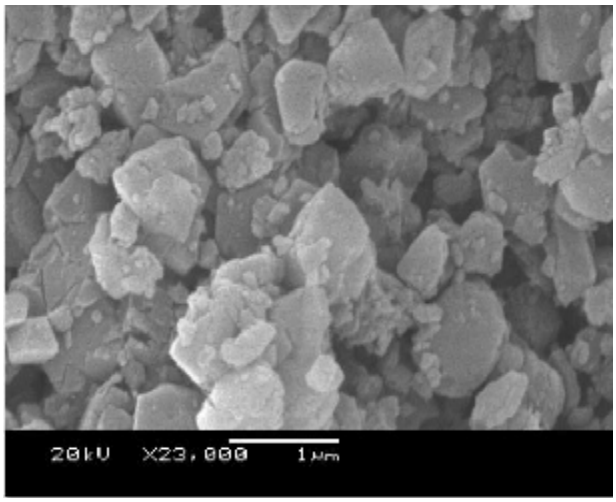

Figure (7) SEM image of (Pt-Ni-Co) / SBA-15 at a magnificationof 10,000.

Although EDAX is a good method for approximating the elements composition of catalysts, composition of SBA-15 from EDAX analysis is (O 53.77% and Si 46.23%) while the composition of 1% (Pt-Ni-Co)/SBA-15 is (O 56.27%, Si 42.75%, Co 0.46% and Ni 0.52%). Themetal loaded catalyst is tested and no traces of the Ptmetal were identified. This is due to the unreliability of EDAX when small percentages of metal (smaller than 1 wt% for Pt, Ni and Co) are present as the area EDAX is performed over may not be sufficiently large enough to identify the presence of these metal clusters. This and the uneven distribution of these metal clusters both hinder the identification of their presence by EDAX.

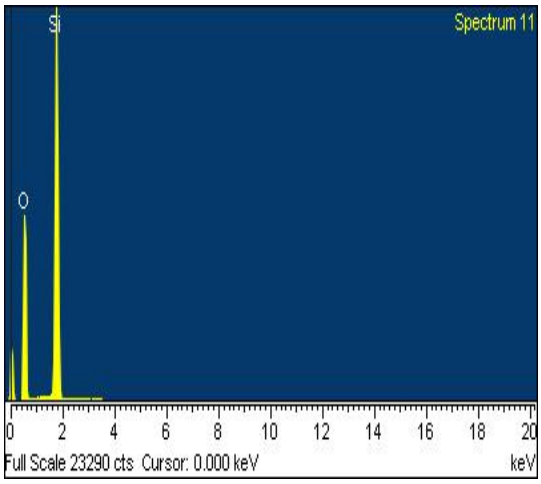

Figure (8) Typical EDAX image for SBA-15.

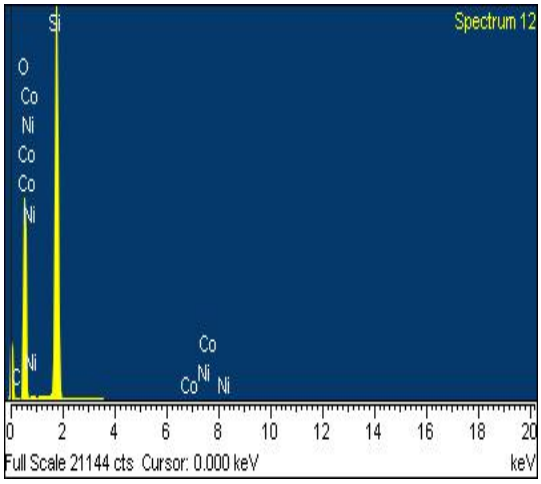

Figure (9) Typical EDAX image for 1% (Pt-Ni-Co) / SBA-15.

Figure (10) shows the TEM images of 1% (Pt-Ni-Co)/SBA-15 sample which is taken for the catalyst after post-testing. It is evident from the TEM image; which prove valuable demonstrating structural of the catalyst where the hexagonal pore structure and orderly pore arrangement could be clearly observed. The long-range order and mesoporous structure arrays were disturbed significantly after 1% (Pt-Ni-Co)/SBA-15 doping by grafting incipient witness impregnation.

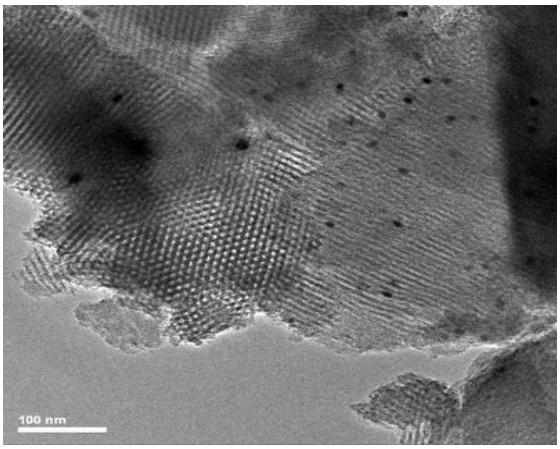

Figure (10) TEM images of 1% (Pt-Ni-Co)/SBA-15at 100 nm.

The structure of 1% (Pt-Ni-Co)/SBA-15 in Figure (10) consists of long cylindrical pores running parallel to each other in the same direction for a section of the catalyst. Most significantly of this image, is the view of the catalyst along the side of and down the centre of the pores, this exemplifies the structure of SBA-15 shown in the schematic Figure (1).

TEM can be used to identify metal structure distribution on catalysts. It is clear from Figure (10) the metal cluster size and distribution of the groups of metals

atoms on the 1% (Pt-Ni-Co)/SBA-15catalysts, as seen in Table (1). From observing the TEM image it is clear that the metal clusters are better dispersed and this agrees with literature [38] resulting in a larger surface area for the reaction to take place.

Conversion of n-heptane

The total conversion in wt. % was calculated for the1% (Pt-Ni-Co)/SBA-15 catalyst at each temperature maintaining a constant flow rate of 20-45 ml min^{-1} from the following Equation.

$$Conversion\ (n.C\ 7\ wt\%) = \frac{[n\ C_7\ in\ (g)] - [n\ C_7\ out\ (g)]}{[n\ C_7\ in\ (g)]} \times 100\%$$

Figure (11) shows the calculated conversion for the 1% (Pt-Ni-Co)/SBA-15 tested catalyst at different temperatures for a constant n-C_7 flow rate of 0.287 ml min^{-1}. The SBA-15 catalysts do show activity which results from the presence of Lewis acid sites within the structure of the catalyst. 1% (Pt-Ni-Co)/SBA-15 demonstrates the next highest conversion at higher temperatures with a conversion (around 85%) at 400 ^{o}C. Tri-metallic 1% (Pt-Ni-Co)/SBA-15 may be found to have higher activity due to the metal cluster size.

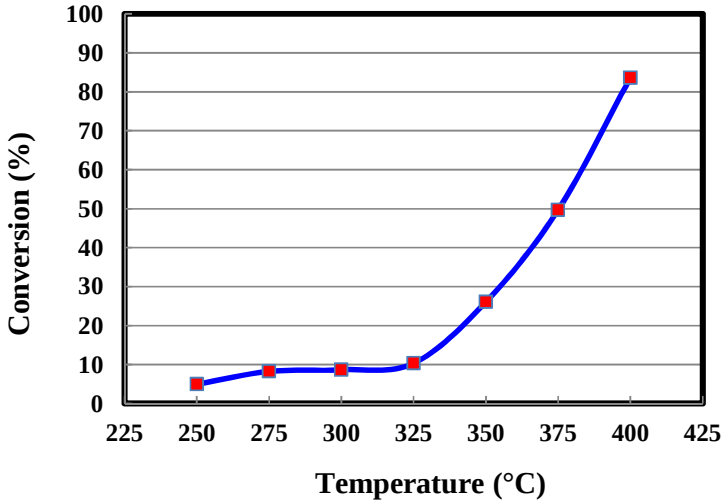

Figure (11) Conversion of n-heptane for the1% (Pt-Ni-Co)/ SBA-15 tested catalyst.

Selectivity to Isomerisation

The selectivity to isomerisation products (i-C7) for (Pt-Ni-Co)/SBA-15 catalyst at the different tested temperatures was calculated from the product yields (g) in following equation.

$$Selectivity\ to\ Isomerisation\ (wt\%) = \frac{\sum i - C_7(g)}{\sum Total\ Products(g)} \times 100\%$$

Figure (12) displays the selectivity to isomerisation products for 1% (Pt-Ni-Co)/SBA-15 catalyst at different operating temperatures. The Brønsted acid sites of the zeolite allow for the transformation of intermediate alkenes into their structural isomers during the reaction mechanism for isomerisation over bi-functional catalysts. Without these acid sites, as on SBA-15, only dehydrogenation and hydrocracking reactions can occur [38].

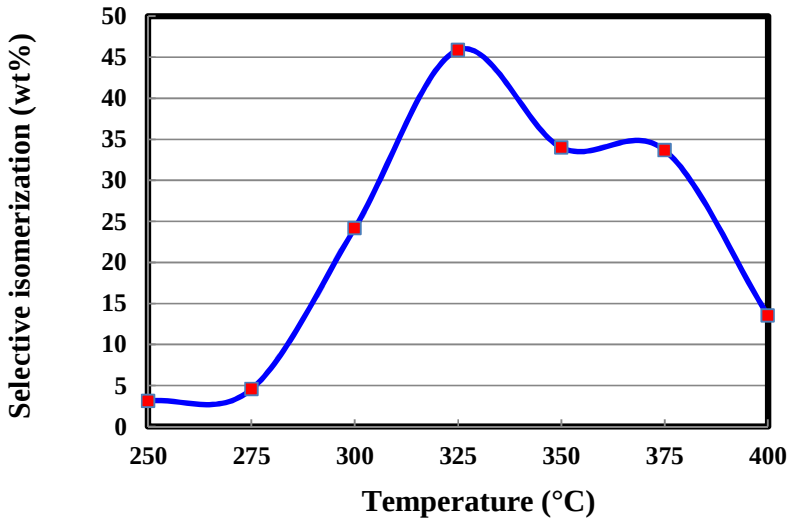

Figure (12)Isomerisation product selectivity for the tested catalysts.

The larger SBA-15 catalyst pores result in poor selectivity to isomerisation products and are therefore not product selective. For example, cyclohexane with a molecular diameter of 0.6 nm is 10 times smaller than the pore diameter of SBA-15 with 6.5 nm, therefore the reactant molecules react and exit the catalysts pores before any selectivity can occur [39].

Selectivity to Cracking

The selectivity to cracked products ($C_1 - C_6$) was calculated for the1%(Pt-Ni-Co) / SBA-15 catalyst at all the tested temperatures for an n-C_7flow rate of 0.287 $mlmin^{-1}$ by equation

$$Selectivity\ to\ Cracking\ (wt\%) = \frac{\sum Cracked\ Product\ (g)}{\sum Total\ Products(g)} \times 100\%$$

Figure (13) displays the results for the selectivity to cracking for the 1% (Pt-Ni-Co) / SBA-15 catalyst at tested temperatures.

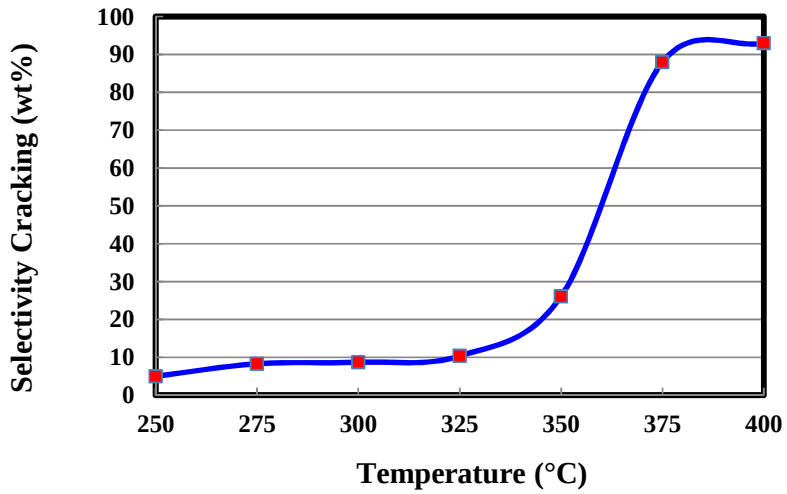

Figure (13) Cracking product selectivity for the tested catalysts.

From this graph it is evident that the selectivity to cracking on 1% (Pt-Ni-Co) / SBA-15 show an increase in selectivity of up to 90 wt % at 400^{o}C. Here the SBA-15 catalysts exhibit a greater selectivity for cracked products, again due to their pore structure and the presence of Lewis acid sites on the catalyst. Although the SBA-15 catalysts are active, as they are not structurally selective to desired isomerisation products for the hydroisomerisation of n-C_7 and have no Brønsted acid sites which aid isomerisation. Hydroisomerisation reactions occur in thermodynamic equilibrium with hydrocracking reactions as seen in literature [40] and typically occur at relatively low temperatures of 210-270^{o}C. The SBA-15 catalysts are not active at the low temperatures required for hydroisomerisation and therefore display no selectivity to isomerisation products. However the SBA-15 catalysts show high selectivity for cracked products due to the high operating temperatures of 300 – 400 ^{o}C and again due to the presence of Lewis acid sites within the structure of the catalyst.

CONCLUSIONS

1. The pore size of SBA-15 was found to be 8.5 nm. This led to good dispersion of metals and increased the metal sites available for reaction and therefore affected the activity of the catalyst.
2. SBA-15 was found to have no shape selectivity towards isomerisation products due to its large pores relative to isomerisation products and lack of Brønsted acid sites.
3. 1% (Pt-Ni-Co)/SBA-15 catalyst samples showed good selectivity to cracked products due to the existence of Lewis acid sites on the catalysts.
4. The activity of the tri-metallic 1% (Pt-Ni-Co)/SBA-15 catalyst was found to be rather good. The presence of Pt,Ni and Co enhances the distribution of the metals clusters and therefore allows for a greater surface area available for reaction.
5. The selectivity of isomerization is not high, so further studies have to be carried out in the future.

ACKNOWLEDGEMENTS

Dr. Talib M. Albayati is grateful to the University of Technology, in Republic of Iraq, for allowing postdoctoral leave and to Manchester Metropolitan University, in British United Kingdom (UK), for financial support.

REFERENCES

[1]. Chen, C.Y. X. Ouyang, S.I. Zones, S.A. Banach, S.A. Elomari, T.M. Davis, A.F. Ojo. Characterization of shape selective properties of zeolites via hydroisomerization of n-hexane. Microporous and Mesoporous Materials 164 (2012) 71–81.

[2]. Steijns, M, Froment GF, Jacobs P, Uytterhoven P, Weitkamp J. Hydroisomerization and hydrocracking. 2. Product distributions from ndecaneand n-dodecane. IndustEng Prod Res Dev20 (1981) 654–60.

[3]. Campelo JM, Lafont F, Marinas M. Hydroisomerization and hydrocracking of nheptaneon Pt/SAPO-5 and Pt/SAPO-11 catalysts. J Catal156 (1995)11–8.

[4]. Akhmedov VM, Al-Khowaiter SH. Recent advances and future aspects in theselective isomerization of high n-alkanes. Catal Rev 49 (2007) 33–139.

[5]. Deldari H. Suitable catalysts for hydroisomerization of long-chain normalparaffins. ApplCatal A Gen 293 (2005)1–10.

[6]. Ono Y. A survey of the mechanism in catalytic isomerization of alkanes. CatalToday 81 (2003)3–16.

[7]. Belloum M, Travers C, Bournonville JP. Isomerization of C4–C7 paraffins onzeolitic catalysts (bibliographic review). Oil Gas SciTechnol46 (1991) 89–107.

[8]. Martens JA, Jacobs JA, Weitkamp J. Attempts to rationalize the distribution ofhydrocracked products. I qualitative description of the primary hydrocrackingmodes of long chain paraffins in open zeolites. App Catal20 (1986) 239–81.

[9]. Martens JA, Tielen M, Jacobs PA. Relation between paraffin isomerizationCapability and pore architecture of large-pore bifunctional zeolites. Stud SurfSciCatal46 (1989) 49–60.

[10]. Ledoux, M.J.; Del Gallo, P.; Pham-Huu, C.; York, A.P.E. Molybdenum oxycarbide isomerization catalysts for cleaner fuel production. *Catal. Today* 27(1996) 145-150.

[11]. Blekkan, E.A.; Pham-Huu, C.; Ledoux, M.J.; Guille, J. Isomerization of *n*-heptane on an oxygenmodified molybdenum carbide catalyst. *Ind. Eng. Chem. Res.* 33 (1994) 1657-1664.

[12]. Ledoux, M.J.; Guille, J.; Pham-Huu, C.; Blekkan, E.A.; Peschiera, E. Process for the isomerisation of straight hydrocarbons containing at least 7 carbon atoms using catalysts with a base of molybdenum oxycarbide. U.S. Patent 5, 576 (1996),466,.

[13]. Chica A, Corma A. Hydroisomerization of pentane, hexane, and heptane for improving the octane number of gasoline. J Catal, 187(1): (1999) 167－176.

[14].Pope T D, Kriz J F, Stanciulescu M, Nonnier J. A study of catalyst formulations for isomerization of C7 hydrocarbons. ApplCatal A, 233 (2002) 45－62.

[15]. Marme F, Coudurier G, Védrine J C. Acid-type catalytic properties of heteropolyacid H3PW12O40 supported on various porous silica-based materials. MicroporMesopor Mater, 22 (1998)151－163.

[16]. Nowinska N, Fiedorov R, Adamiec J. Catalytic activity of supported heteropoly acids for reactions requiring strong acid centers. J ChemSoc Faraday Trans, 87 (1991) 749－753.

[17]. Chimienti M E, Pizzio L R, Cáceres C V, Blanco M N. Tungstophosphoric and tungstosilicic acids on carbon as acidic catalysts. ApplCatal A, 208 (2001) 7－19.

[18]. Kozhevnikov I V, Sinnema A, Janse R J J. New acid catalyst comprising heteropoly acid on a mesoporous molecular sieve MCM-41. CatalLett, 30 (1995)241－252.

[19]. Liu Q Y, Wu W L, Wang J, Ren X Q, Wang Y R. Characterization of 12-tungstophosphoric acid impregnated on mesoporous silica SBA-15 and its catalytic performance in isopropylation of naphthalene with isopropanol. MicroporMesopor Mater, 76 (2004) 51－60.

[20]. Mukai S R, Shimoda M, Lin L, Tamon H, Masuda T. Improvement of the preparation method of "ship-in-the-bottle" type 12-molybdophosphoric acid encaged Y-type zeolite catalysts. ApplCatal A, 256 (2003) 107－113.

[21]. Sulikowski B, Rachwalik R. Catalytic properties of heteropoly acid/zeolite hybrid materials: Toluene disproportionation and transalkylation with 1,2,4-trimethylbenzene. ApplCatal A, 256 (2003) 173－182.

[22]. Sulikowski B, Haber J, Kubacka A. Novel "ship-in-the-bottle" type catalyst: Evidence for encapsulation of 12-tungstophosphoric acid in the supercage of synthetic faujasite. CatalLett,39 (1996) 27－31.

[23]. Wang, J.A. L.F. Chen, L.E. Norena, J. Navarrete, M.E. Llanos, J.L. Contreras, O.Novaro, Mesoporous structure, surface acidity and catalytic properties of Pt/Zr–MCM-41 catalysts promoted with 12-tungstophosphoric acid. Microporous and Mesoporous Materials 112 (2008) 61–76.

[24]. McVicker, G.B. P.J. Collins, J.J. Ziemack, Model compound reforming studies: A comparison of alumina-supported platinum and iridium catalysts. Journal of Catalysis 74 (1982) 156–172.

[25]. Wang, J.A. X.L. Zhou, L.F. Chen, L.E. Norena, G.X. Yu, C.L. Li,Hydroisomerization of n-heptane on the Pt/$H_3PW_{12}O_{40}$/Zr-MCM-41 catalysts. Journal of Molecular Catalysis A: Chemical 299 (2009) 68–76.

[26]. Zhao, D. J. Feng, Q. Huo, N. Melosh, G.H. Fredrickson, B.F. Chmelka, G.D. Stucky, Triblock copolymer syntheses of mesoporous silica with periodic 50–300 angstrom pores, Science 279 (1998) 548–552.

[27]. Zhao, D., Huo, Q., Feng, J., Chmelka, B.F. and Stucky, G.D. ‘‘Nonionic triblock and star diblock copolymer and oligomeric surfactant syntheses of highly ordered, hydrothermally stable, mesoporous silica structures’’, J. Am. Chem. Soc., 120(1998) 6024–6036.

[28]. Beck J S, Vartuli J C, Roth W J, Leonowicz M E, Kresge C T, Schmitt K D, Chu C T W, Olson D H, Sheppard E W, McCullen S B, Higgins J B, Schlenker J L. *J Am Chem Soc*,114 (1992) 10834.

[29]. Li, X., Liu, X., Ma, Y., Li, M., Zhao, J., Xin, H., Zhang, L., Yang, Y., Li, C., Yang, Q. Engineering the Formation of Secondary Building Blocks within the Hollow Interiors, Advanced Materials, 24 (2012) 1424-1428.

[30]. John N. Kuhn, Wenyu Huang, Chia-KuangTsung, Yawen Zhang, and Gabor A. Somorjai , Structure Sensitivity of Carbon-Nitrogen Ring Opening: Impact of PlatinumParticle Size from below 1 to 5 nm upon Pyrrole Hydrogenation Product Selectivity over Monodisperse Platinum Nanoparticles Loaded onto Mesoporous Silica. Journal American Chemical Society, 130(2008)14026-14027.

[31]. Kruk, M. M. Jaroniec, A. Sayari,Influence of hydrothermal restructuring conditions on structural properties of mesoporous molecular sieves. Chem. Mater. 11 (1999) 492–500.

[32]. JamilehTaghavimoghaddam, Gregory P. Knowles, Alan L. Chaffee. Preparation and characterization of mesoporous silica supported cobalt oxide asa catalyst for the oxidation of cyclohexanol, Journal of Molecular Catalysis A: Chemical 358 (2012) 79– 88.

[33]. Chiu, J. J., Pine, D. J., Bishop, S. T., Chmelka, B. F. Friedel–Crafts alkylation properties of aluminosilica SBA-15 meso/macroporous monoliths and mesoporous powders, Journal of Catalysis, 221(2004) 400-412.

[34]. Tsoncheva, T. L. Ivanova, C. Minchev, M. Fröba, Cobalt-modified mesoporousMgO. ZrO_2 and CeO_2 oxides as catalysts for methanol decomposition. Journal of Colloidand Interface Science. 333 (2009) 277–284.

[35]. Zhou, L. J. Xu, H. Miao, F. Wang, X. Li,Catalytic oxidation of cyclohexane to cyclohexanol and cyclohexanone over Co_3O_4nanocrystals with molecular oxygen. Applied Catalysis A: General 292 (2005) 223–228.

[36].Junming Du, HualongXu, Jiang Shen, Jingjing Huang, Wei Shen, Dongyuan Zhao. Catalytic dehydrogenation and cracking of industrial dipentene over M/SBA-15(M = Al, Zn) catalysts.Applied Catalysis A: General 296 (2005) 186–193.

[37]. Zhaohua Luan, Jay A. Fournier. In situ FTIR spectroscopic investigation of active sites and adsorbate interactions in mesoporousaluminosilicate SBA-15 molecular sieves. Microporous and Mesoporous Materials 79 (2005) 235–240.

[38].Eswaramoorthi,I., Lingappen, N. Ni-Pt/H-Y Zeolite Catalysts for Hydroisomerisation of n-C6 and n-C7, Cat Let, 87 (2003) 133-142.

[39]. Dwyer, J. Zeolite Structure, Composition and Catalysis. Chemistry and Industry, (1984) 258-269.

[40]. Karthikeyan, D., Lingappan, N., Sivasankar, B.Hydroisomerisation of n-octane over bifunctional Ni-Pd/HY zeolite catalysts, Industrial Engineering Chemical Resource, 47 (2008) 6538-6546.